Carbohydrate Research 343 (2008) 2650–2656

Contents lists available at ScienceDirect

Carbohydrate Research

journal homepage: www.elsevier.com/locate/carres

Secondary relaxations in supercooled and glassy sucrose–borate aqueous solutions

M. Paula Longinotti [a], Horacio R. Corti [b,*], Juan J. de Pablo [c]

[a] Gerencia de Química, Comisión Nacional de Energía Atómica, Av. General Paz 1499 (1650) San Martin, Buenos Aires, Argentina
[b] Departamento de Física de la Materia Condensada, Comisión Nacional de Energía Atómica, Av. General Paz 1499 (1650) San Martín, Buenos Aires and Instituto de Química Física de los Materiales, Medio Ambiente y Energía (INQUIMAE), Facultad de Ciencias Exactas y Naturales, Universidad de Buenos Aires, Pabellón II, Ciudad Universitaria, Av. Int. Cantilo s/n (1428) Buenos Aires, Argentina
[c] Department of Chemical and Biological Engineering, University of Wisconsin, 1415 Engineering Drive, Madison, WI 53706, USA

ARTICLE INFO

Article history:
Received 28 April 2008
Received in revised form 24 July 2008
Accepted 2 August 2008
Available online 9 August 2008

Keywords:
T_g-scaling
Dielectric relaxation
Molecular mobility
Carbohydrates
Supercooled aqueous solutions
Aqueous glasses

ABSTRACT

The dielectric relaxation spectra of concentrated aqueous solutions of sucrose–borate mixtures have been measured in the supercooled and glassy regions in the frequency range of 40 Hz to 2 MHz. The secondary (β) relaxation process was analyzed in the temperature range 183–233 K at water contents between 20 and 30 wt %. The relaxation times were obtained, and the activation energy of that process was calculated. In order to assess the effect of borate on the relaxation of disaccharide–water mixtures, we also studied the dielectric behavior of sucrose aqueous solutions in the same range of temperatures and water contents. Our findings support the view that, beyond a water content of approximately 20 wt %, the secondary relaxation of water–sucrose and water–sucrose–borate mixtures adopts a universal character that can be explained in terms of a simple exponential function of the temperature scaled by the glass transition temperature (T_g). The behavior observed for water–sucrose and water–sucrose–borate mixtures is compared with previous results obtained in other water–carbohydrate systems.

1. Introduction

The properties of aqueous solutions of carbohydrates are of considerable interest because of their ubiquity and wide range of applications. Water-soluble carbohydrate polymers are the most widely used among the biopolymers in industry, and sugar–water solutions provide simple models of food systems[1] and have a well-documented cryoprotectant capacity.[2] In spite of their importance, the solvation characteristics of sugars in water have received little attention for years, as pointed out by Franks and Grigera[3] in their 1990 review on solution properties of carbohydrates. The supercooled and glassy regions of these systems, which are of particular interest in the stabilization of food and pharmaceutical products and in the cryopreservation areas of technology,[4] are still not well understood.[5]

The dynamics of aqueous solutions of carbohydrates in the supercooled and glassy states has been studied using Quasi-elastic neutron spectroscopy,[6] RMN,[7–9] and molecular dynamics.[10–12] The dielectric relaxation spectroscopy, which permits access to a wide time domain range, was applied for the first time by Suggett and co-workers[13,14] and later by Johari and co-workers.[15]

Several authors[13,14,16–21] have studied the dielectric relaxation of water-rich solutions (water contents higher than 30 wt %) in the high frequency range (above 1 MHz), where the contribution to the relaxation is essentially due to the hydroxylic groups of water and the saccharide. Other measurements have been performed at frequencies lower than 1 MHz[15,22–27] in the saccharide-rich region (water contents lower than 30 wt %).

Two relaxation processes were observed in aqueous solutions of saccharides, as in other glass forming liquids: a slow α-relaxation, only observed above the glass transition temperature (T_g), due to the cooperative rearrangements of the molecules, and a fast β-relaxation, which extends below T_g.

The nature of the β-process in the saccharide-rich region of saccharide–water mixtures has been a matter of controversy ever since the first data were reported. Chan et al.[15] argued that the motion of water molecules is only partially responsible for the β-relaxation, while Moran et al.,[24] based on NMR studies of anhydrous glucose and glucose 75 wt %,[8,24] suggested that the motion of the hydroxymethyl groups should not be used to explain the fast β-relaxation. Recent studies by Swenson and co-workers[26,27] on glucose, fructose, and sucrose aqueous solutions with water contents between 20 and 30 wt % led these authors to propose that

* Corresponding author. Tel.: +54 11 6772 7174; fax: +54 11 6772 7886.
E-mail addresses: hrcorti@cnea.gov.ar (H. R. Corti), depablo@engr.wisc.edu (J. J. de Pablo).

0008-6215/$ - see front matter © 2008 Elsevier Ltd. All rights reserved.
doi:10.1016/j.carres.2008.08.003

the β-relaxation in these mixtures is mainly due to hydration water.

Sucrose, as well as other disaccharides, is a natural osmolyte produced by cells to protect biomolecules against the effects of freezing, low water activity, and other harsh conditions.[28,29] Its dielectric properties in aqueous solutions have been studied in the past in the water-rich region,[14,17,20] and more recently in the sucrose-rich region.[25–27] It is also known[30,31] that the addition of sodium tetraborate (borax) and other oxyanions to aqueous sucrose results in the formation of esters, thereby reducing component mobility and improving protein or cell stability in co-lyophilized oxyanion–disaccharide matrices.[32–34]

In spite of their technological and biological significance, the dynamics of disaccharide–oxyanion mixtures have not been measured before. In this work, we present a dielectric relaxation study of aqueous systems containing sucrose, borate, and water (between 20 and 30 wt %). The measurements were performed in the range of temperature from 183 K to 293 K, and frequencies between 40 Hz and 2 MHz. The aim of this study is to generate information pertaining to the dynamics of the β-relaxation in the sub-T_g and supercooled regimes, and to compare the behavior of the aqueous sucrose to that of sucrose–borate solutions over the same range of water content and temperature. Our results extend the β-relaxation map obtained by Champion et al.[25] and Swenson and co-workers[26,27] for highly concentrated sucrose–water mixtures to water–sucrose–borate mixtures, and help us to rationalize the role of water and borate in such systems.

2. Experimental

2.1. Sample preparation

Sucrose and sodium tetraborate decahydrate ($Na_2B_4O_7{\cdot}10H_2O$) were obtained from Fluka and Aldrich, respectively, and were used without further purification. Water was deionized and passed through a Millipore filter.

Aqueous sucrose–borate mixtures were prepared in screw-topped Pyrex flasks by adding preweighted amounts of borate to known quantities of water to prepare supersaturated salt solutions. The resulting mixtures were heated until complete dissolution of the salt and added to the corresponding amounts of sugar needed to obtain the desired borate–sugar concentrations. The resulting mixtures were heated again until complete dissolution of the sugar. Two sets of aqueous borate–sucrose solutions of constant water content (20 or 30 wt %) were prepared.

The maximum boron fraction in each set of solutions was limited by caramelization reactions, since color development was favored at high borate and sucrose concentrations.

Aqueous sucrose solutions (20, 25, and 30 wt % water content) were prepared in a similar way as sucrose–borate–water mixtures.

Table 1
Concentration (sucrose and borax weight fraction, and sugar and boron molar fraction) and glass transition temperature of the sucrose–borate (SB) and sucrose (S) aqueous solutions

Sample	w_S	w_{Borax}	x_S	x_{Boron}	T_g (K)
S1	0.700	—	0.109	—	201.3
S2	0.750	—	0.136	—	212.9
S3	0.800	—	0.174	—	227.0
SB1	0.8008	0.0018	0.1757	0.0026	227.2
SB2	0.7962	0.0045	0.1725	0.0066	227.6
SB3	0.7741	0.0153	0.1585	0.0213	228.8
SB4	0.6726	0.0263	0.1023	0.0272	206.9
SB5	0.6590	0.0402	0.0991	0.0411	208.5

The concentrations of all species in the sucrose and sucrose–borate solutions, given in weight and molar fraction for comparison, are summarized in Table 1.

The onset glass transition temperatures of the sucrose–borate aqueous solutions (samples SB1–SB5) reported in Table 1 were determined by differential scanning calorimetry (DSC) using a Mettler 822 and STARe Thermal Analysis System version 6.1 software (Mettler Toledo AG, Switzerland). The instrument was calibrated using standard compounds (indium, zinc, and lead) of well-defined melting point and heat of melting. The glass transition temperatures of the sucrose aqueous solutions reported in Table 1 correspond to the fit of the onset transition temperatures reported in the literature by using the Gordon and Taylor equation[35] as informed in a recent work.[36]

2.2. Dielectric cell and set up

The dielectric measurements were performed with an Agilent 4294-A Impedance Analyzer in the frequency range of 40 Hz to 2 MHz. The 4294-A covers a wider frequency range (40 Hz to 110 MHz), but parasitic impedances limited our measurements to frequencies lower than 2 MHz.

The dielectric cell, constructed in our laboratory, was based on a design by Hollingworth and Saville,[37] in which the large distance between the liquid region and the edge of the cell suppressed electric field fringing. The cell consists of two cylindrical copper electrodes (48 mm diameter and 10 mm thick), separated by an acrylic spacer of 2 mm thickness. To create the sample chamber, a circular hole (8 mm diameter) was made in the middle of the spacer. The ratio between the radii of the spacer and the sample region is equal to 6, ensuring the suppression of edge effects. Two small holes drilled through the edge of the spacer to the sample chamber, allowed filling the chamber and keeping it completely filled during the entire experiment, despite any volume changes in the sample produced by the temperature variations. The electrode surfaces in contact with the sample were wet polished with silicon carbide and aluminum oxide up to 0.3 μm and, afterwards, a thin film of gold was vacuum deposited over these surfaces.

The temperature was controlled using the setup shown in Figure 1. A 10-L Dewar containing liquid nitrogen (A) was connected

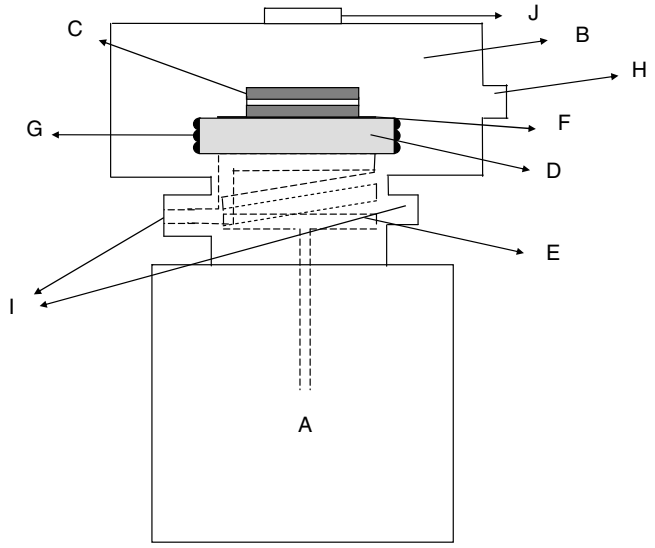

Figure 1. Diagram of the liquid nitrogen accessory used for temperature control: (A) nitrogen Dewar; (B) vacuum chamber; (C) dielectric cell; (D) metal plate; (E) tube immersed in the Dewar for cooling the plate D; (F) thin film of mica; (G) heater resistance; (H) vacuum-proof holes for electrical connections; (I) connections to the vacuum pump; (J) optical window.

to a vacuum chamber (B), which contained the dielectric cell (C) located over a metal plate (D) that was cooled by pumping nitrogen through a tube (E), with one end immersed in the Dewar and the other end connected to a vacuum pump (I). The vacuum pump was also connected to the cell chamber by a two-way valve. Therefore, before pumping liquid nitrogen into the plate, a vacuum was created over the cell chamber that prevented vapor condensation over the dielectric cell surface. The electric insulation between the plate and the dielectric cell was provided by a thin film of mica (F).

The plate (D) contained two holes, one for a platinum resistance and another for a heater resistance (G). The temperature in the cell was controlled by a Lakeshore 330 Temperature Controller, which supplied a power output to the heater proportional to the temperature difference between the platinum resistance and the set up temperature. The temperature of the sample was read with a calibrated platinum resistance placed in a hole made in one of the electrodes near the sample chamber.

The cell chamber contained vacuum-proof holes (H) for the output of the electrical connections of the Lakeshore 330 with the heater and platinum resistances, and for the dielectric cell with the Impedance Analyzer.

2.3. Cell calibration and dielectric measurements

The dielectric measurements were made by applying an AC voltage of 0.5 V to the dielectric cell. A residual capacitance of 31–35 pF and a frequency-dependent conductance lower than 4 μS represent the impedance contributions of the plastic spacer contained between the electrodes. These contributions were systematically taken into account in the determination of the dielectric properties of the sample by considering an equivalent circuit where the capacitance and resistance of the acrylic spacer are in parallel with the corresponding impedance components of the sample.

The cell constant was determined between 223.2 K and 298.2 K by measuring the cell capacitance with the empty cell and the cell filled with anhydrous glycerol. As the static dielectric constant of anhydrous glycerol is known in this temperature range,[38] the determination of the static capacitance difference between the cell filled with glycerol and the empty cell gave the cell constant value. This value varied from $38.4 \pm 0.4\ m^{-1}$ at 298.2 K to $39.7 \pm 0.7\ m^{-1}$ at 223.2 K, and agrees within the error with the geometrical value ($40 \pm 4\ m^{-1}$) at room temperature. The dependence of the cell constant with temperature was fitted using a linear regression.

The correct choice of the proposed equivalent circuit was verified by comparing the dielectric spectrum of glycerol measured in this work between 203.2 and 293.2 K, with the results obtained by Schneider et al.[39]

For the measurement of aqueous sucrose–borate and sucrose solutions, the dielectric cell was filled with the corresponding solution and placed in the vacuum chamber of the liquid nitrogen accessory. Vacuum was applied for 30 min before cooling the cell to 183.2 K. After the desired temperature was reached, the sample cell was kept for 30 min at that temperature before the frequency scan was performed. The cell was then heated to a temperature 10 K higher, and the same protocol was applied until a temperature of 293.2 K was attained. The cell geometry and the high viscosity of the studied solutions ensured that the applied vacuum did not change the composition of the solution.

The temperature and concentration ranges covered in this study include the supercooled and glassy regions of the supplementary phase diagram of sucrose aqueous solutions as shown in Figure 2. The effect of the added borate on T_g is important but it does not modify the qualitative aspects of the phase diagram. Therefore, the supercooled and glassy regions were also investigated for the sucrose–borate system.

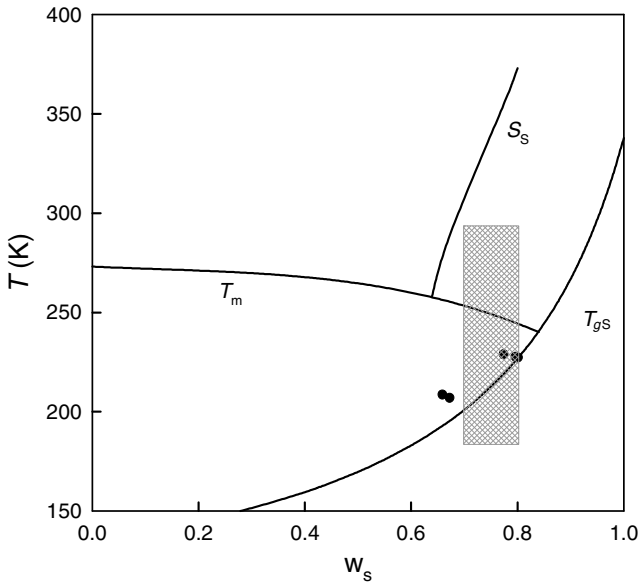

Figure 2. Supplemented phase diagram of the sucrose–water mixture showing the equilibrium curves for the liquid–solid transitions, the non-equilibrium glass transition temperature, and the region (gray box) where the dielectric relaxation study was performed. The filled circles correspond to the glass transition temperatures of the sucrose–borate samples SB1–SB5.

In the temperature range where only one relaxation process was observed and polarization of the electrodes was absent, the complex dielectric constant, $\varepsilon^*(f) = \varepsilon'(f) - i\varepsilon''(f)$, was fitted with Eq. 1:

$$\varepsilon^* = \varepsilon_\infty + \left(\frac{\Delta\varepsilon_\beta}{1 + (i\omega\tau_\beta)^h}\right) - i\frac{\sigma}{\varepsilon_0\varpi} \quad (1)$$

where σ is the conductivity of the sample, ε_0 is the permittivity of the vacuum, $\Delta\varepsilon_\beta$ is the dielectric increment of the β-process, τ_β is the relaxation time of the same process, $\omega = 2\pi f$ is the angular frequency, and the exponent h reflects the width of the Cole–Cole[40] relaxation processes. This function has been used to describe the secondary dielectric relaxation for many other systems.[41,42]

At higher temperatures, Eq. 1 did not describe adequately the dielectric dispersion and relaxation spectra, since the α-relaxation and the polarization of the electrodes contributed to these spectra in the low frequency limit. Besides, separation of these two contributions was not possible, considering the limited frequency range covered in this work.

3. Results

3.1. Analysis of the dielectric relaxation of sucrose solutions

The dielectric losses as a function of temperature at constant frequency of the sucrose solutions having water concentrations 20, 25, and 30 wt % were measured. The isochrones (fixed frequency, $f = 5$ kHz) curves ($\log \varepsilon''$ vs T) exhibit two peaks; the one above T_g, which corresponds to the α-relaxation, is stronger than the peak close to T_g, which is associated with the β-relaxation. At higher frequencies, the β-relaxation peaks shift to higher temperatures and merge with the primary relaxation peaks. Only the β-relaxation process was analyzed in this work.

The parameters corresponding to the fits performed using Eq. 1 are reported in Table 2. Figure 3 shows, as a way of example, the dispersion and relaxation spectra of aqueous sucrose with

Table 2
Conductivity, β-relaxation times, and other parameters obtained by fitting $\varepsilon^*(\omega)$ with Eq. 1 for sucrose–borate and sucrose aqueous solutions

	T (K)	$\log(\sigma/\mathrm{S\ m^{-1}})$	ε_∞	$\log(\tau_\beta/\mathrm{s})$	h_β	$\Delta\varepsilon_\beta$
S1	183.2	−11.0	5.0	−3.49	0.41	40.4
	193.2	−8.0	5.1	−4.38	0.42	39.5
	203.2	−8.0	4.8	−5.16	0.41	46.6
	213.2	−7.5	0.9	−5.80	0.35	61.5
S2	183.2	−8.5	4.7	−2.74	0.36	37.4
	193.2	−8.2	4.8	−3.72	0.38	32.8
	203.2	−9.1	4.9	−4.47	0.39	32.3
	213.2	−8.2	4.7	−5.21	0.39	36.8
	223.2	−7.4	3.1	−5.88	0.37	46.8
S3	193.2	−11.2	5.2	−1.61	0.30	37.3
	203.2	−14.7	5.4	−3.28	0.34	23.8
	213.2	−15.9	5.7	−4.13	0.38	21.1
	223.2	−12.6	6.0	−4.78	0.40	20.8
	233.2	−12.3	6.5	−5.40	0.42	22.7
	243.2	−8.0	6.0	−5.92	0.40	29.4
SB1	193.2	−11.7	6.1	−2.18	0.31	32.7
	203.2	−11.2	6.4	−3.54	0.35	24.5
	213.2	−9.1	6.7	−4.33	0.39	22.9
	223.2	−8.2	6.9	−4.83	0.40	23.9
	233.2	−7.6	6.9	−5.37	0.39	27.5
SB2	183.2	−15.4	5.1	−1.27	0.30	26.6
	193.2	−12.9	5.2	−2.24	0.31	26.4
	203.2	−12.5	5.3	−3.31	0.34	23.2
	213.2	−13.1	5.5	−4.19	0.37	21.3
	223.2	−12.4	5.7	−4.82	0.39	21.8
	233.2	−8.4	5.7	−5.37	0.38	25.2
SB3	183.2	−11.5	5.0	−1.31	0.28	29.2
	193.2	−16.0	5.0	−2.18	0.28	28.2
	203.2	−15.6	5.4	−3.84	0.35	19.7
	213.2	−9.9	5.6	−4.44	0.37	20.4
	223.2	−8.8	5.6	−4.88	0.37	23.0
SB4	183.2	−12.5	7.9	−3.27	0.37	32.1
	193.2	−9.0	7.9	−3.97	0.37	34.7
SB5	183.2	−8.7	6.5	−3.16	0.35	21.1
	193.2	−11.8	6.6	−3.96	0.37	22.0

25 wt % water concentration. The solid lines correspond to the results obtained by fitting ε' and ε'' with Eq. 1, which reproduces correctly the experimental data.

The conductivity values reported in Table 2 are only indicative. Their uncertainties are large in comparison with the dielectric relaxation strength and they do not show a systematic behavior with temperature. Although, as expected, the general trend of the conductivity is to increase with temperature and decrease with sugar concentration.

The β-relaxation times reported in Table 2 are in good agreement with recent data by Swenson and co-workers[26] for sucrose solutions with 25 and 30 wt % water concentrations. The temperature dependence of the β-relaxation time follows a typical Arrhenius behavior:

$$\tau = \tau_0 \cdot \exp\left(\frac{E_a}{RT}\right) \quad (2)$$

where E_a is the activation energy and τ_0 is the value of the relaxation time extrapolated to infinite temperature. The values of E_a and τ_0 obtained for the samples S1–S3 are reported in Table 3 and the relaxation times as a function of the inverse temperature are plotted in Figure 4, together with data reported by Jansson et al.[26]

3.2. Analysis of the dielectric relaxation of sucrose–borate solutions

Figure 5 shows the dielectric relaxation spectra of aqueous sucrose and aqueous borate–sucrose solutions with 30 wt % water concentration at 183.2 and 193.2 K.

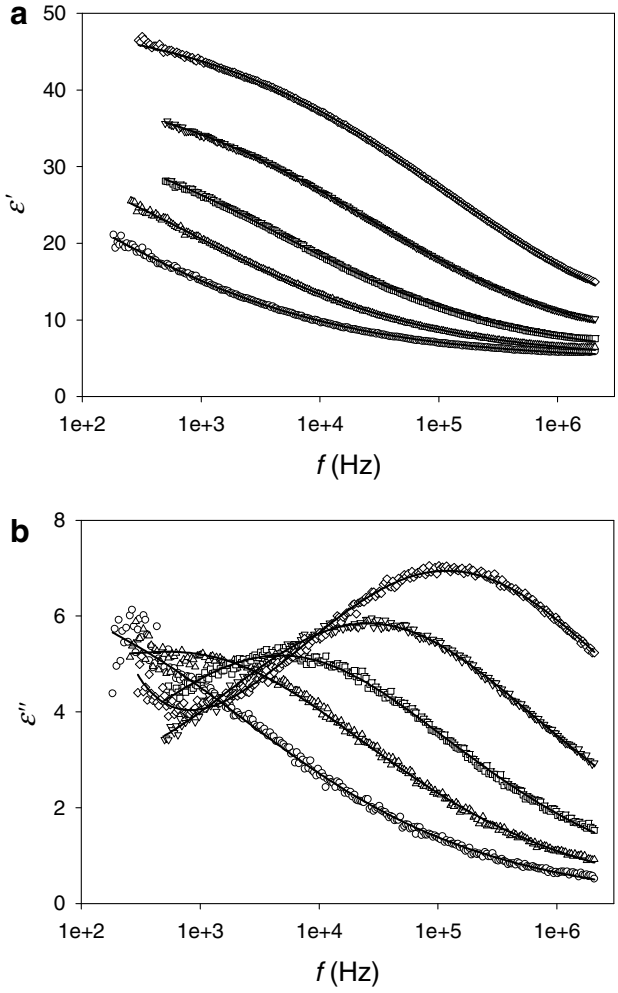

Figure 3. Dielectric dispersion (a) and relaxation spectra (b) of S2 at (○) 183.2 K, (△) 193.2 K, (□) 203.2 K, (▽) 213.2 K, (◇) 223.2 K. The solid lines correspond to the fits of ε' and ε'' (ω) performed with Eq. 1.

Table 3
Arrhenius parameters for the β-relaxation processes in aqueous sucrose and sucrose-borate solutions

Sample	$\log(\tau_0/\mathrm{s})$	E_a (kJ mol^{-1})
S1	−20.0 ± 0.3	58 ± 1
S2	−20.1 ± 0.2	60.9 ± 0.9
S3	−22 ± 2	74 ± 6
SB1	−20 ± 2	67 ± 7
SB2	−21 ± 1	68 ± 2
SB3	−22 ± 2	74 ± 8

The parameters obtained by fitting the β-relaxation in aqueous borate–sucrose solutions with Eq. 1 are reported in Table 2 and the corresponding curves, for SB4 and SB5, are plotted in Figure 5. As it was previously mentioned for sucrose aqueous solutions, the β-relaxation time for sucrose–borate aqueous solutions follows Eq. 2 with τ_0 and E_a values reported in Table 3.

The value of h_β obtained for the secondary process varies between 0.3 and 0.4, with h_β values similar to the ones reported for sucrose aqueous solutions and for a glucose water solution with 25 wt % water concentration.[24] It can be observed that h_β increases slightly with temperature, as observed in sucrose aqueous solutions and other carbohydrate–water mixtures, indicating that the relaxation is more stretched at lower temperatures.

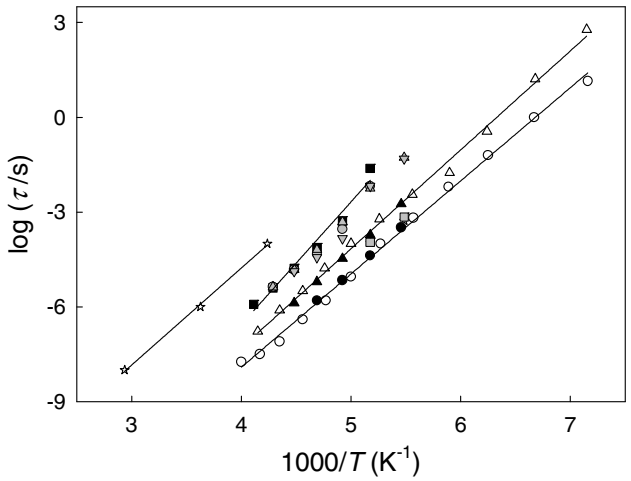

Figure 4. Arrhenius plot of the β-relaxation times of sucrose and sucrose–borate aqueous solutions obtained in this work: (●) S1, (▲) S2, (■) S3, (●) SB1, (▲) SB2, (▼) SB3, (★) SB4, (■) SB5. Data reported by Swenson and co-workers[26] for sucrose aqueous solutions with 30 (○) and 25 (△) wt % of water and by Champion et al.[25] (☆) for 1 wt % water content are also plotted. The solid lines correspond to the Arrhenius fits of the data obtained in this work and others for aqueous sucrose.

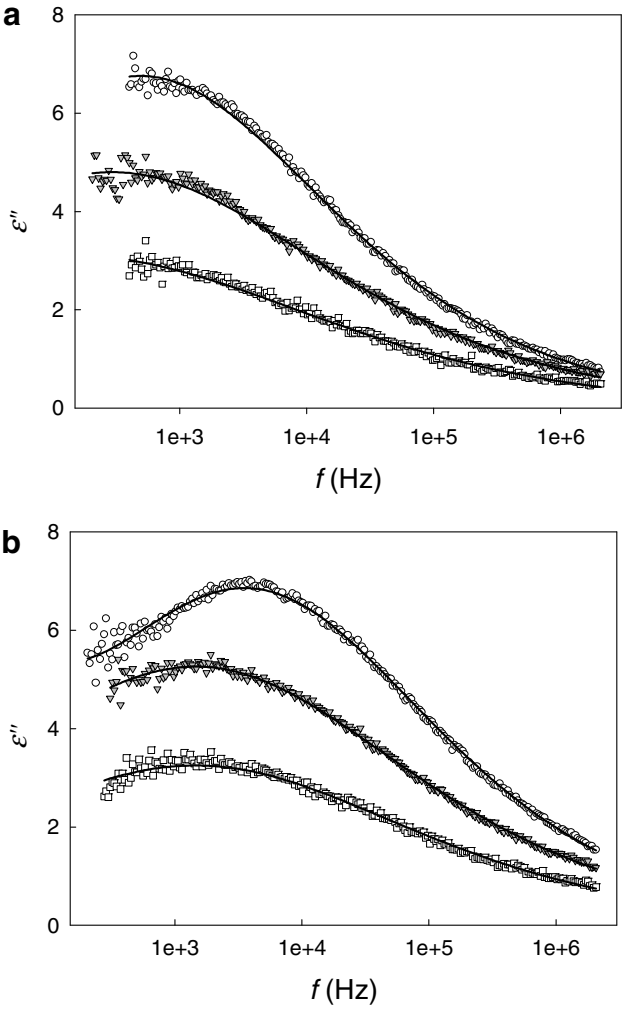

Figure 5. Dielectric relaxation spectra of (○) S1, (▼) SB4, and (□) SB5 at 183.2 (a) and 193.2 K (b). The solid lines correspond to the fits of $\varepsilon''(\omega)$ performed with Eq. 1.

Oh et al.[43] noted that, as it occurs with this study, h_β increases with temperature for glucose solutions containing 3–15 wt % of water and reaches a constant value close to 0.7 at high temperatures. They also observed that h_β increases slightly with the content of water as observed here and as noted by Jansson et al.[26] in carbohydrate-rich biological materials.

The results reported in Table 2 suggest that the addition of borate does not change significantly neither the β-relaxation time nor the magnitude of the relaxation process ($\Delta\varepsilon_\beta$) of the sucrose solutions with 20 wt % of water. On the other hand, in the samples with 30 wt % of water and higher borate–disaccharide molar ratio, the β-relaxation in sucrose–borate aqueous solutions is slower than that corresponding to the sucrose solution. What is more, the magnitude ($\Delta\varepsilon_\beta$) of the relaxation process decreases with borate content, as can be observed in Figure 5.

4. Discussion

It is observed that, in both the sucrose and the sucrose–borate solutions at constant temperature, an increase in the concentration of sucrose slows down the β-relaxation (Fig. 4). In an attempt to rationalize this behavior, we analyzed the change of the β-relaxation times with temperature by resorting to a T_g-scaled Arrhenius plot ($\log\tau$ vs T_g/T). In this way, the differences in β-relaxation times with concentration level off and the behavior observed in Figure 6 emerges. The Arrhenius plots for the β-relaxation times merge onto a common line for the three sucrose and the five sucrose–borate aqueous solutions studied in this work, covering the supercooled ($T_g/T < 1$) and the glassy regions ($T_g/T > 1$). Note, however, that the β-relaxation times reported by Champion et al.[25] for the 1 wt % water content sucrose solution deviate from this common line.

This behavior was also observed for other carbohydrate–water mixtures, as shown in Figures 7 and 8 for glucose and maltose, respectively, where a common relaxation time is observed for all samples of constant at T_g/T values, at water concentrations above 15 wt %. Below this water concentration, the relaxation time at constant T_g/T decreases with water content.

β-Relaxation times shown in Figure 7 were obtained from data reported by Chan et al.[15], Noel et al.,[22,44] and Moran et al.[24] The T_g values of glucose aqueous solutions were calculated with the Gordon and Taylor equation[35] using experimental onset-T_g data

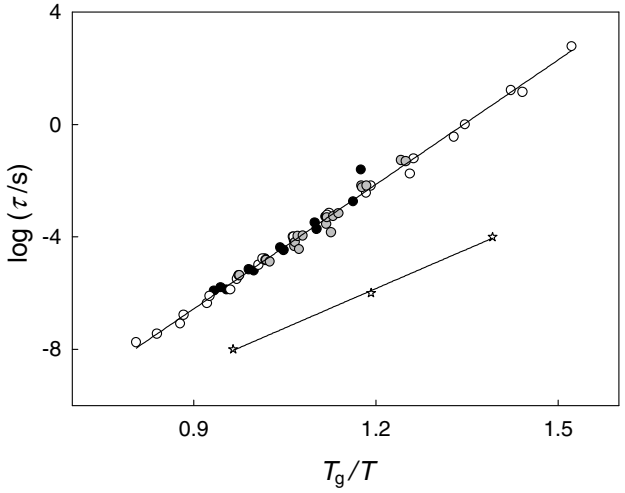

Figure 6. T_g-scaled Arrhenius plot for the dielectric relaxation times of sucrose and sucrose–borate aqueous solutions: S1–S3 (●), SB1–SB5 (●), data reported by Swenson et al.[26] on sucrose aqueous solutions with 30 and 25 wt % water content (○) and by Champion et al.[25] for aqueous sucrose with 1 wt % water concentration (☆).

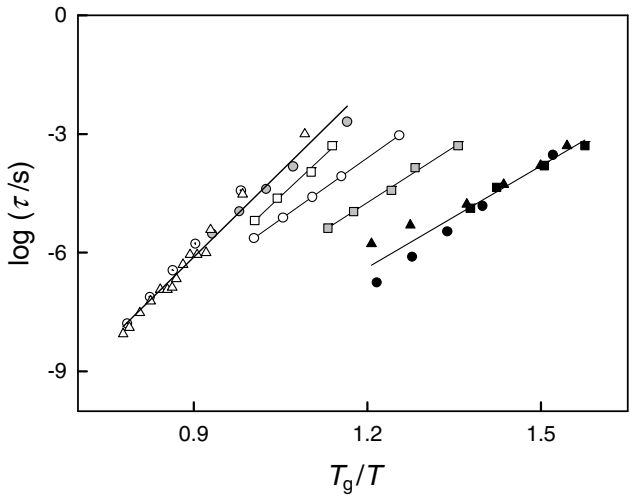

Figure 7. T_g-scaled Arrhenius plot for the dielectric relaxation times of glucose aqueous solutions. β-Relaxation times for 0 wt % water content reported by Chan et al.[15] (●), Noel et al.[44] (▲), and Noel et al.[22] (■). Glucose aqueous solution with 5 wt % (▩),[22] 10 wt % (○),[15] 12 wt % (□),[22] 15 wt % (◍),[15] 25 wt % (△),[24] and 30 wt % (⊙)[15] water concentrations.

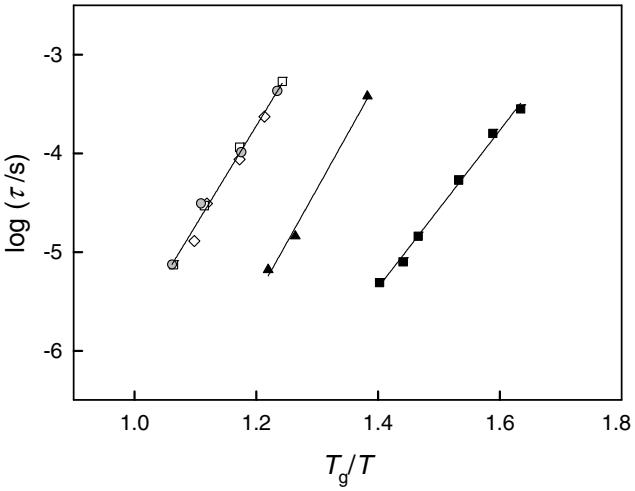

Figure 8. T_g-scaled Arrhenius plot for the dielectric relaxation times of maltose aqueous solutions. β-Relaxation times for water concentrations: 0 wt % (■), 7 wt % (▲), 15 wt % (◇), 19 wt % (□), and 23 wt % (◍), reported by Noel et al.[22]

reported by Luyet and Rasmussen,[45] and Roos and Karel.[46] Relaxation times plotted in Figure 8 correspond to data reported by Noel et al.[22] with T_g values calculated with the Gordon and Taylor equation[35] using experimental onset-T_g data reported by Green and Angell,[47] and Roos.[48]

Considering the systems studied in this work, the mean value of the activation energy of the secondary relaxation of sucrose and sucrose–borate aqueous solutions for water contents between 20 and 30 wt % is around 70 ± 13 kJ mol^{-1} (see Table 3). Similar values were reported for other concentrated solutions of saccharides in water. Noel et al.[23] reported activation energies of 59 kJ mol^{-1} for glucose 90 wt % and 62 kJ mol^{-1} for maltose 90 wt %. They also found that the activation energy decreases with water content, reaching values of 42 kJ mol^{-1} for dry glucose and 45 kJ mol^{-1} for dry maltose. Although these values are not in agreement with those reported for glucose by Chan et al.,[15] a detailed analysis of the literature suggests that this behavior is common to all the saccharides for which data are available. In sucrose/water mixtures the activation energy of the β-process decreases from approximately 64 kJ mol^{-1} for water contents between 20 and 30 wt % to 50 kJ mol^{-1} for 1 wt % water.[25]

As it can be observed in Figures 6–8, the situation for β-relaxation at water concentrations below 15 wt % is different from the observed behavior at water contents between 15 and 30 wt %. This water content limit coincides with the water percolation concentration obtained by coarse grain molecular dynamics simulations performed by Molinero et al.[12,49] These authors found that water forms extended clusters in the carbohydrate matrix that percolate at water contents between 10 and 18 wt % for sucrose–water mixtures[49] and at 18 wt % for glucose–water solutions.[12]

If we assume that the β-relaxation is due to both relaxation of the hydration water interacting with the saccharide and the saccharide itself at low water contents, it is reasonable to expect that the motions of the water molecules are determined by the saccharide packing since water clusters are isolated among them. The addition of the first one or two water molecules to the dry saccharide leads to a growing water cluster structure, with relaxation times that become faster at constant temperature. However, when these relaxation times are compared at the same T_g/T value, the relaxation rate diminishes with water addition.

At water contents above approximately 15 wt %, the addition of water varies the relaxation times, which remain constant when they are scaled by the glass transition temperature. Therefore, it can be thought that once the water cluster structure percolates, the addition of water to the system at constant T_g/T does not modify the β-relaxation time. In this region, the addition of water at constant temperature (decreasing T_g) or the increase of temperature at constant water content leads to a decrease of T_g/T, and consequently an increase in the relaxation rate.

The fact that the β-relaxation of sucrose–borate solutions scales with T_g/T in the same way as the sucrose solutions implies that the higher preservation ability of formulations containing borate, when compared at constant temperature, could be simply due to their higher glass transition temperature. That is, at the same temperature, a sugar solution containing borate and the same water concentration has a higher T_g/T value and, consequently, the β-relaxation is slower and so is the mobility of reactants that participate in deterioration reactions.

The addition of borate to aqueous sucrose solutions also decreases the strength of the β-relaxation ($\Delta\varepsilon_\beta$), probably due to the decrease in the number of molecules capable to orient in an electric field (water molecules hydrating the borate ions and the –OH and –CH_2OH groups of the disaccharide forming esters with the borate ions).[50]

In the case of proteins, Cicerone and co-workers[51,52] have recently shown that protein dynamics are strongly coupled to the solvent dynamics in the glassy state; the higher the fluctuations in the matrix, the higher the conformational fluctuations in the protein. Therefore, the dielectric studies of aqueous solutions of sugar and other polyols near the glass transition could provide a useful comparative test of the stabilization power of such systems.

5. Conclusions

We have analyzed the secondary (β) dielectric relaxation of aqueous sucrose solutions and sucrose–borate mixtures in the range of water concentration from 20 to 30 wt %, and have observed a common behavior when the dielectric relaxation time is scaled according to the glass transition temperature. The β-relaxation times reported for sucrose solutions at a water content of 1 wt % show that the relaxation rates, when scaled with T_g, are considerably faster than those corresponding to solutions having higher water contents. We propose that this change of behavior

with water content arises for water concentrations close to the percolation values reported by molecular dynamics, and can therefore be explained in terms of the formation of the water structure.

We found that the addition of borate to aqueous sucrose solutions does not alter the β-relaxation behavior when plotted in terms of a scaled temperature T_g/T. We therefore propose that the efficacy of the disaccharide–borate mixtures for protein stabilization is partly due to an increase of the T_g.

Acknowledgements

The authors thank financial support from CNEA (Project P5 PID 36-3), University of Buenos Aires (Project X-220), CONICET (PID 5977) and the University of Wisconsin Materials Research Science and Engineering Center on Nanostructured Interfaces. M.P.L. thanks doctoral fellowship from the Consejo Nacional de Investigaciones Científicas y Técnicas (CONICET).

References

1. Slade, L.; Levine, H. *Pure Appl. Chem.* **1988**, *60*, 1841–1864.
2. Fahy, G. M.; Levy, D. I.; Ali, S. E. *Cryobiology* **1987**, *24*, 196–213.
3. Franks, F.; Grigera, J. R. Solution Properties of Low Molecular Weight Polyhydroxy Compounds. In *Water Science Reviews 5*; Felix, Franks, Ed.; Cambridge University Press, 1990.
4. Brumfiel, G. *Nature* **2004**, *428*, 14–15.
5. Kilburn, D.; Townrow, S.; Meunier, V.; Richardson, R.; Alam, A.; Ubbink, J. *Nat. Mater.* **2006**, *5*, 632–635.
6. Branca, C.; Magazù, S.; Maisano, G. *Chem. Phys.* **2003**, *292*, 341–345.
7. Moran, G. R.; Jeffrey, K. R. *J. Chem. Phys.* **1999**, *110*, 3472–3483.
8. van Dusschoten, D.; Tracht, U.; Heuer, A.; Spiess, H. W. *J. Phys. Chem. A* **1999**, *103*, 8359–8364.
9. van den Dries, I. J.; van Dusschoten, D.; Hemminga, M. A. *J. Phys. Chem. B* **1998**, *102*, 10483–10489.
10. Roberts, C. J.; Debenedetti, P. G. *J. Phys. Chem. B* **1999**, *103*, 7308–7318.
11. Ekdawi-Sever, N. C.; Conrad, P. B.; de Pablo, J. J. *J. Phys. Chem. A* **2001**, *105*, 734–742.
12. Molinero, V.; Çağin, T.; Goddard, W. A., III. *J. Phys. Chem. A* **2004**, *108*, 3699–3712.
13. Tait, M. J.; Suggett, A.; Franks, F.; Ablett, S.; Quickenden, P. A. *J. Solution Chem.* **1972**, *1*, 131–151.
14. Suggett, A.; Clark, A. H. *J. Solution Chem.* **1976**, *5*, 1–15.
15. Chan, R. K.; Pathmanathan, K.; Johari, G. P. *J. Phys. Chem.* **1986**, *90*, 6358–6362.
16. Mashimo, S.; Miura, N.; Umehara, T. *J. Chem. Phys.* **1992**, *97*, 6759–6765.
17. Saito, A.; Miyawaki, O.; Nakamura, K. *Biosci., Biotechnol., Biochem.* **1997**, *61*, 1831–1835.
18. Matsuoka, T.; Okada, T.; Murai, K.; Koda, S.; Nomura, H. *J. Mol. Liquids* **2002**, *98–99*, 317–327.
19. Weingärtner, H.; Knocks, A.; Boresch, S.; Höchtl, P.; Steinhauser, O. *J. Chem. Phys.* **2001**, *115*, 1463–1472.
20. Fuchs, K.; Kaatze, U. *J. Chem. Phys.* **2002**, *116*, 7137–7144.
21. Fuchs, K.; Kaatze, U. *J. Phys. Chem. B* **2001**, *105*, 2036–2042.
22. Noel, T. R.; Parker, R.; Ring, S. G. *Carbohydr. Res.* **1996**, *282*, 193–206.
23. Noel, T. R.; Parker, R.; Ring, S. G. *Carbohydr. Res.* **2000**, *329*, 839–845.
24. Moran, G. R.; Jeffrey, K. R.; Thomas, J. S.; Stevens, J. R. *Carbohydr. Res.* **2000**, *328*, 573–584.
25. Champion, D.; Maglione, M.; Niquet, G.; Simatos, D.; Le Meste, M. *J. Therm. Anal. Calorim.* **2003**, *71*, 249–261.
26. Jansson, H.; Huldt, C.; Bergman, R.; Swenson, J. *Phys. Rev. E* **2005**, *71*, 011901-1–011901-7.
27. Jansson, H.; Bergman, R.; Swenson, J. *J. Non-Cryst. Solids* **2005**, *351*, 2858–2863.
28. Rumsey, S. C.; Galeano, N. F.; Arad, Y.; Deckelbaum, R. J. *J. Lipid Res.* **1992**, *33*, 1551–1561.
29. Sun, W. K.; Leopold, A. C.; Crowe, L. M.; Crowe, J. H. *Biophys. J.* **1996**, *70*, 1769–1776.
30. Miller, D. P.; de Pablo, J. J.; Corti, H. R. *J. Phys. Chem. B* **1999**, *103*, 10243–10249.
31. Izutsu, K.; Rimando, A.; Aoyagi, N.; Kojima, S. *Chem. Pharm. Bull.* **2003**, *51*, 663–666.
32. Miller, D. P.; Anderson, R. E.; de Pablo, J. J. *Pharm. Res.* **1998**, *15*, 1215–1221.
33. Ekdawi-Sever, N.; Goentoro, L. A.; de Pablo, J. J. *J. Food Sci.* **2003**, *68*, 2504–2511.
34. Ohtake, S.; Schebor, C.; Palecek, S. P.; de Pablo, J. J. *Cryobiology* **2004**, *48*, 81–89.
35. Gordon, M.; Taylor, J. S. *J. Appl. Chem.* **1952**, *2*, 493–500.
36. Longinotti, M. P.; Corti, H. R. *J. Phys. Chem. Ref. Data* **2008**, *37*, 1503–1515.
37. Hollingsworth, A. D.; Saville, D. A. *J. Colloid Int. Sci.* **2003**, *257*, 65–76.
38. Davidson, D. W.; Cole, R. H. *J. Chem. Phys.* **1951**, *19*, 1484–1490.
39. Schneider, U.; Lunkenheimer, P.; Brand, R.; Loidl, A. *J. Non-Cryst. Solids* **1998**, *235–237*, 173–179.
40. Cole, K. S.; Cole, R. H. *J. Chem. Phys.* **1941**, *9*, 341–351.
41. Döß, A.; Paluch, M.; Sillecu, H.; Hinze, G. *Phys. Rev. Lett.* **2002**, *88*, 095701-1–095701-4.
42. Minoguchi, A.; Kitai, K.; Nozaki, R. *Phys. Rev. E* **2003**, *68*, 031501-1–031501-7.
43. Oh, J.; Seo, J.; Kim, H. K.; Hwang, Y. *J. Non-Cryst. Solids* **2006**, *352*, 4679–4684.
44. Noel, T. R.; Ring, S. G.; Whittam, M. A. *J. Phys. Chem.* **1992**, *92*, 5662–5667.
45. Luyet, B.; Rasmussen, D. *Biodynamica* **1968**, *10*, 167–191.
46. Roos, Y.; Karel, M. *Cryo-Letters* **1991**, *12*, 367–376.
47. Green, J. L.; Angell, C. A. *J. Phys. Chem.* **1989**, *93*, 2880–2882.
48. Roos, Y. *Carbohydr. Res.* **1993**, *238*, 39–48.
49. Molinero, V.; Çağin, T.; Goddard, W. A., III. *Chem. Phys. Lett.* **2003**, *377*, 469–474.
50. Longinotti, M. P.; Corti, H. R. *J. Solution Chem.* **2004**, *33*, 1029–1040.
51. Cicerone, M. T.; Soles, C. L. *Biophys. J.* **2004**, *86*, 3836–3845.
52. Caliskan, G.; Mechtani, D.; Roh, J. H.; Kisliuk, A.; Sokolov, A. P.; Azzam, S.; Cicerone, M. T.; Lin-Gibson, S.; Peral, I. *J. Chem. Phys.* **2004**, *121*, 1978–1983.